A HYDRO-MECHANIC VIBRATION ABSORBER WITH ADJUSTABLE OPERATING FREQUENCY

Helmut Kogler*, Bernd Winkler, Andreas Plöckinger

Linz Center of Mechatronics GmbH, Altenberger Straße 69, 4040 Linz, Austria
*Corresponding author: Tel.: +43 732 2468 6059; E-mail address: helmut.kogler@lcm.at

---

ABSTRACT

Unwanted resonances in industrial plants often result in unpleasant noise or may even end up in a reduced lifetime of mechanical structures and components. Such vibrations are often reduced by well-established vibration absorbers, which are designed and precisely tuned to one specific frequency. Furthermore, often the natural frequency of, for instance, a mechanical structure is not accurately known and must be identified by an experimental modal analysis. Another limitation of conventional single-frequency absorbers is that in some applications the frequency of the unwanted vibrations varies over lifetime, which reduces the effectiveness of the initially designed absorber. Moreover, in many cases the frequency of the undesirable vibration changes with the operating point of the plant, which requires the installation of multiple vibration absorbers with different operating frequencies. In this paper a new hydro-mechanical vibration absorber with a continuously adjustable operating frequency is presented, which eliminates the shortcomings mentioned above. In contrast to conventional absorbers the stiffness of the hydro-mechanical spring mass absorber is realized by a gas-loaded hydraulic capacitance, which depends on the mean operating pressure. The concept of the presented absorber is investigated theoretically and validated by simulation experiments. The results are discussed in detail and an outlook on further steps in development is provided.

Keywords: vibration, resonance, mitigation, adaptive, hydraulic, absorber

---

1. INTRODUCTION

Most industrial processes are characterised by a cyclic operation. The inevitable reaction forces often result in generally unwanted vibrations in the basements, suspensions or housings of the plant. The vibrations typically appear in the range from below one cycle per second up to several hundred Hertz, like for instance due to unbalance effects in high speed rotors. In some cases the vibrations may act as an excitation for other dynamical mechanical systems located close to the actual working process. Furthermore low frequency resonances of buildings and bridges may result from broad band excitation effects like earthquakes or wind gusts. If the frequency of the excitation is close to or even coincide with the natural frequency of an exposed dynamic system, then the vibration may cause a tremendous resonance effect, which may lead to either undesirable noise or even to a reduced life time of the machine or structure. There even exist a few cases, where some specific operating points of a machine result in a structural instability, which may end up in the worst case of a destruction of the plant.

As a counter measure against such unwanted resonance effects so-called vibration absorbers are widely used, which basically represent an oscillating system acting against the resonance of a vibrating primary system or structure, see for instance [1, 2, 3, 4, 5, 6]. Most vibration absorbers are able to operate at a single frequency and, thus, are designed for one specific working point. Therefore, the natural frequency of the absorber must fulfill certain conditions for the desired suppression of the vibrations. For many decades researchers developed numerous strategies for an optimized absorber

design. The most relevant methodology often used as a reference is presented in [7]. Other publications from recent years dealing with design optimization can be found, for instance, in [8, 9, 10], where in the latter also energy harvesting with a vibration absorber is discussed.

In fact, the natural frequency of the primary system can be identified accurately by more or less laborious measurements, however, the perfect tuning can often only achieved by an absorber with variable frequency. For instance, in [11] an adaptive vibration absorber with smart leaf springs is presented, where the stiffness of the absorber is controlled by the bending of the leaf springs. Another contribution dealing with a vibration absorber with adjustable inertia using a cone based continuously variable transmission can be found in [12]. Also in [13] an active vibration absorber with adjustable frequency using an electromagnetic actuator assembled at the end of a cantilever beam is investigated, and a similar approach is presented in [14]. The specific problem of a varying natural frequency of the primary system due to different working conditions is discussed in [15] by the use of multiple tuned mass dampers for a parallel machining robot.

In this paper the concept of a hydro-mechanical vibration absorber (HMA) with adjustable operating frequency is investigated by theoretic considerations. The basic design aspects with regard to optimal tuning and damping are based on the established literature [7]. Furthermore, simulations carried out with an exemplary parameter set confirm the expected functionality. Moreover, not only the mitigation effect for a weakly damped primary system is shown, also the applicability for moderate instabilities is presented.

2. BASIC CONCEPT OF THE HYDRO-MECHANIC VIBRATION ABSORBER

The basic functional scheme of an adaptive vibration absorber is illustrated in Fig. 1a attached to a primary damped spring mass oscillator (m_P, k_P, c_P) resonating due to a harmonic excitation force F. The absorber mass m_A is interconnected to the mass m_P of the primary system by a combination of two springs and a damper. Beside a constant spring coefficient $\overline{k}_M$ an additional variable stiffness $\tilde{k}_H$ is used in order to realize an adjustable resonance frequency of the absorber. In a so-called hydro-mechanic vibration absorber (HMA), as illustrated in Fig. 1b, the absorber mass resonates between two pressure chambers with gas-loaded accumulators. The nonlinear characteristics of the gas springs in the accumulators depend on the mean operating pressure $\overline{p}$ and result in the variable stiffness $\tilde{k}_H$. The hydraulic reactive force of the absorber $F_A = (p_1 - p_2) A_p$ is transmitted by the housing to the primary mass. The housing is pressurized by two directional on/off seat type valves to a constant mean pressure $\overline{p}$, which propagates slowly through the annulus gaps $(A_\odot)$ between the piston and the sleeve from the central chamber to both working chambers. In order to guarantee a proper dynamic operation of the absorber the relation $A_p \gg A_\odot$ of the relevant cross-section areas must be fulfilled. Assuming that the dynamic leakage flow through the annulus gaps $A_\odot$ is negligible, then only the fluid flow through the resistance R_A between the two pressure chambers results in a considerable damping effect.

The hydraulic stiffness of one chamber incorporating the gas-spring of the accumulator reads

$$k_H = \frac{A_p^2 n \overline{p}}{V_A} \left(\frac{p_0^G}{\overline{p}} \right)^{-\frac{1}{n}},$$ (1)

where the compressibility of the oil is neglected for simplicity. Since the displacement of all individual springs k_M and k_H is unique, their interconnection results in a parallel[1] arrangement of springs. Thus,

---

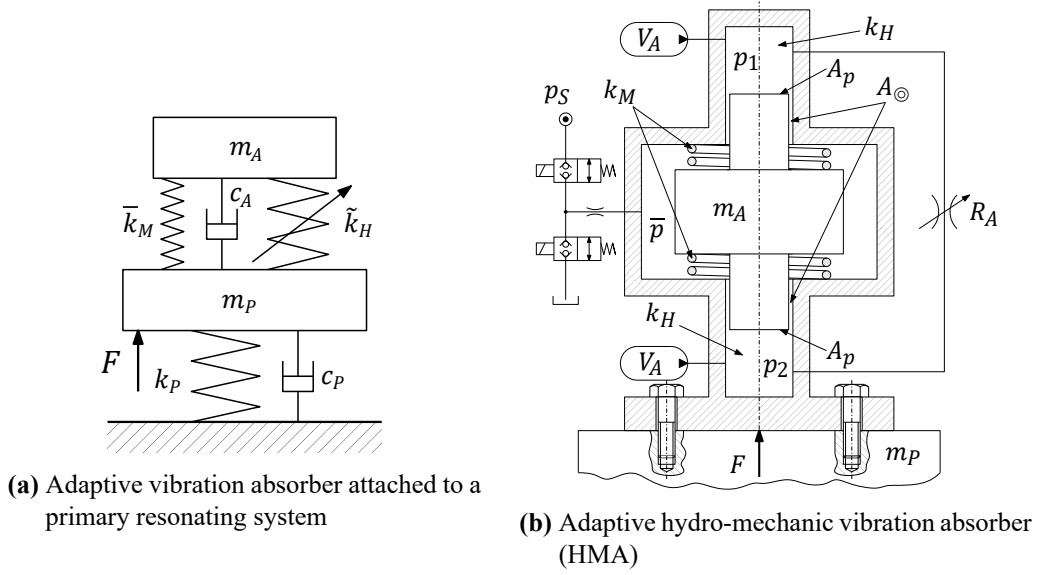[1] In a serial arrangement of multiple springs the force is unique.

(a) Adaptive vibration absorber attached to a primary resonating system

(b) Adaptive hydro-mechanic vibration absorber (HMA)

Figure 1: Adaptive absorber concept

Table 1: Parameters of a reference configuration

Parameter	Value
primary mass	$m_P = 100\,\text{kg}$
primary stiffness	$k_P = 9.87 \cdot 10^6\,\frac{\text{N}}{\text{m}}$
primary resonance frequency	$\omega_P \approx 50 \cdot 2\pi\,\frac{\text{rad}}{\text{s}}$
absorber mass	$m_A = 5\,\text{kg}$
piston diameter	$d_P = 40\,\text{mm}$
accumulator volume	$V_A = 0.3\,\ell$
gas pre-load pressure	$p_0^G = 20\,\text{bar}$
polytropic exponent	$n = 1.3$
hydraulic damping resistance	adjustable

the resonance frequency of the absorber depending on the operating pressure $\overline{p}$ calculates to

$$\omega_A = \sqrt{\frac{\tilde{k}_H + \overline{k}_M}{m_A}} = \sqrt{\frac{2}{m_A}\left(\frac{A_p^2 n \overline{p}}{V_A}\left(\frac{p_0^G}{\overline{p}}\right)^{-\frac{1}{n}} + k_M\right)} \tag{2}$$

and the operating pressure depending on the resonance frequency ω reads

$$\overline{p} = \left(\frac{V_A m_A \left(p_0^G\right)^{\frac{1}{n}}}{2A_p^2 n}\omega^2\right)^{\frac{n}{n+1}}, \tag{3}$$

where k_M is neglected for simplicity. Both relations are illustrated in Fig. 2 for a parameter set according to Tab. 1, which results in an operating range between approximately 25 Hz up to 80 Hz for meaningful pressure values $\overline{p}$.
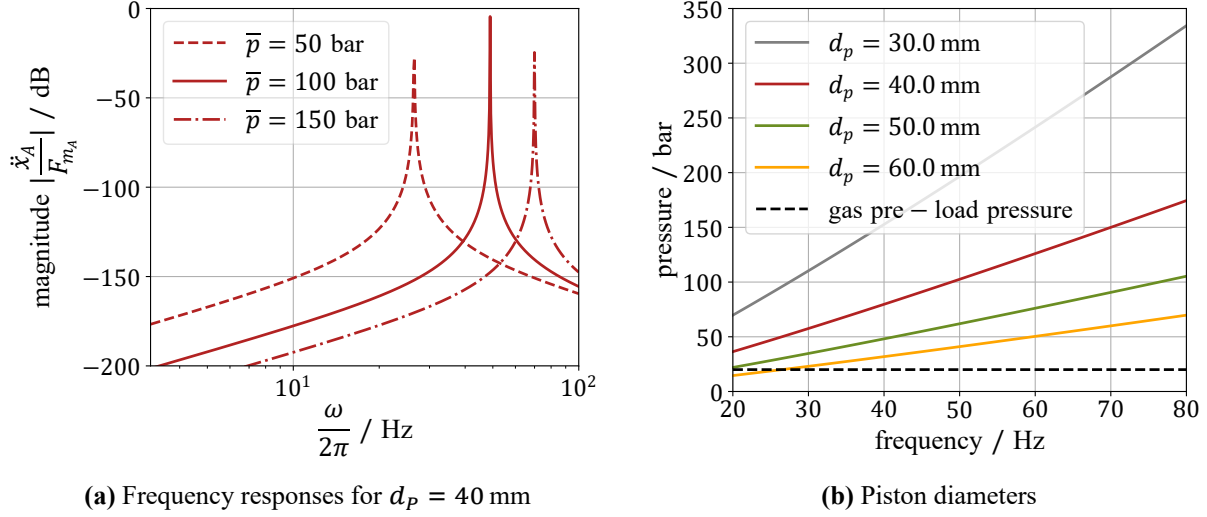
(a) Frequency responses for $d_P = 40$ mm

(b) Piston diameters

Figure 2: Operating range

In Fig. 2b the mean pressure $\overline{p}$ related to the resonance frequency for different piston diameters $d_p = \sqrt{\frac{4A_p}{\pi}}$ is presented. The dashed black line indicates the gas pre-load pressure of the accumulator p_0^G, which must be sufficiently below the minimum operating pressures of both chambers in order to guarantee an appropriate operation. For instance, the absorbers with the parameters according to Tab. 1, but designed with larger piston diameters represented by the green and orange line, respectively, would be too close to or even below the gas pre-load pressure, which means that the accumulators are nearly empty in this frequency range. On the other hand, the design with a piston diameter $d_p = 30$ mm requires a high mean pressure for a high frequency operation, which would result in a too high ratio of operating pressure to pre-load pressure.

3. MODELING

The mathematical model of the adaptive HMA from Fig. 1b reads

$$
\begin{bmatrix} \dot{x}_P \\ \dot{v}_P \\ \dot{x}_A \\ \dot{v}_A \\ \dot{p}_1 \\ \dot{p}_2 \end{bmatrix} =
\begin{bmatrix}
v_P \\
\frac{1}{m_P}\left(A_p\left(p_1 - p_2\right) - c_P v_P - k_P x_P + F\right) \\
v_A \\
\frac{1}{m_A}A_p\left(p_2 - p_1\right) \\
\frac{E_{\mathcal{F}}}{V_A\left(\left(\frac{p_0^G}{p_1}\right)^{\frac{1}{n}}\left(\frac{E_{\mathcal{F}}}{np_1}-1\right)+1\right)}\left(A_p\left(v_A - v_P\right) - \alpha\frac{Q_N}{\sqrt{p_N}}\sqrt{p_1 - p_2}\right) \\
\frac{E_{\mathcal{F}}}{V_A\left(\left(\frac{p_0^G}{p_2}\right)^{\frac{1}{n}}\left(\frac{E_{\mathcal{F}}}{np_2}-1\right)+1\right)}\left(-A_p\left(v_A - v_P\right) + \alpha\frac{Q_N}{\sqrt{p_N}}\sqrt{p_1 - p_2}\right)
\end{bmatrix}
\tag{4}
$$

with the dynamic states x_P, v_P for the position and the velocity of the primary mass, x_A, v_A are the position and the velocity of the absorber mass and p_1, p_2 are the pressure states in the absorber chambers. As mentioned above the mechanical stiffness of the absorber k_M is neglected for simplicity. Furthermore, the cross-sectional areas of the annulus gaps are neglected ($A_\odot = 0$) and, thus, no dynamic leakage is considered. The hydraulic resistance R_A between the absorber's pressure chambers is

considered as a proportional valve orifice (Q_N, p_N) with a square root characteristics and the opening parameter α. The effective compressibility modulus of the fluid is considered with $E_{\mathcal{F}} = 12000\,\text{bar}$. For simplicity no viscous friction of the absorber mass is considered. The system from Eq. (4) will be considered later for the simulations, but for the design analysis a linearized model is used, which calculates to

$$
\begin{bmatrix} \dot{x}_P \\ \dot{v}_P \\ \dot{x}_A \\ \dot{v}_A \\ \dot{p}_1 \\ \dot{p}_2 \end{bmatrix} = \underbrace{\begin{bmatrix} 0 & 1 & 0 & 0 & 0 & 0 \\ -\dfrac{k_P}{m_P} & 0 & 0 & 0 & \dfrac{A_p}{m_P} & -\dfrac{A_p}{m_P} \\ 0 & 0 & 0 & 1 & 0 & 0 \\ 0 & 0 & 0 & 0 & -\dfrac{A_p}{m_A} & \dfrac{A_p}{m_A} \\ 0 & -\dfrac{A_p}{C_A} & 0 & \dfrac{A_p}{C_A} & -\dfrac{1}{R_A C_A} & \dfrac{1}{R_A C_A} \\ 0 & \dfrac{A_p}{C_A} & 0 & -\dfrac{A_p}{C_A} & \dfrac{1}{R_A C_A} & -\dfrac{1}{R_A C_A} \end{bmatrix}}_{\mathbf{A}} \begin{bmatrix} x_P \\ v_P \\ x_A \\ v_A \\ p_1 \\ p_2 \end{bmatrix} + \begin{bmatrix} 0 \\ \dfrac{1}{m_P} \\ 0 \\ 0 \\ 0 \\ 0 \end{bmatrix} F \tag{5}
$$

with the dynamic matrix $\mathbf{A}$ and the excitation force F as an input. The capacitance of the absorber chambers reads

$$
C_A = \frac{V_A}{n\overline{p}} \left(\frac{p_0^G}{\overline{p}} \right)^{\frac{1}{n}} = \frac{k_H}{A_p^2}, \tag{6}
$$

where, as in Eq. (1), the fluid is considered as incompressible ($E_{\mathcal{F}} \to \infty$) compared to the softness of the gas spring in the accumulators for simplicity. The parameter A_p denotes the cross-sectional area of the absorber piston and R_A is the linearized damping resistance between both pressure chambers of the absorber. For simplicity and in accordance with [7] the viscous friction of the primary system c_P is neglected in the design process. Since the cross-sectional areas of the annulus gaps $A_\odot$ are assumed to be zero, thus, the pressure build up in the middle chamber of Fig. 1b and the corresponding damping effect are negligible. Thus, the transfer function of the displacement of the primary system due to the excitation force F follows to

$$
G(s) = \frac{\hat{x}_P}{\hat{F}} = \begin{bmatrix} 1 & 0 & 0 & 0 & 0 & 0 \end{bmatrix} (s\mathbf{E} - \mathbf{A})^{-1} \begin{bmatrix} 0 & \dfrac{1}{m_P} & 0 & 0 & 0 & 0 \end{bmatrix}^{\mathsf{T}}, \tag{7}
$$

which results in a quite long symbolic expression impossible to be presented here. In order to keep the considerations simple the following substitutions $s = i\omega$, $\omega = \omega_P \xi$, $\omega_A = \omega_P \varphi$, $V_A = \dfrac{2A_p^2 n\overline{p}}{m_A \omega_A^2} \left(\dfrac{p_0^G}{\overline{p}} \right)^{-\frac{1}{n}}$, $m_A = m_P \mu$, $k_P = \omega_P^2 m_P$, $\omega_P = \dfrac{c_c}{2m_P}$, $R_A = \dfrac{c_c \zeta}{A_p^2}$ and $c_P = 0$ are used to rewrite this transfer function (7) in a dimensionless form

$$
G(\xi) = \frac{\hat{x}_P}{\hat{F}} \frac{c_c^2}{m_P} = -\frac{4\left(\mu\varphi^2 \xi - 2i\varphi^2 \zeta + 2i\xi^2 \zeta\right)}{\mu\varphi^2 \xi^3 - 2i\mu\varphi^2 \xi^2 \zeta - \mu\varphi^2 \xi - 2i\varphi^2 \xi^2 \zeta + 2i\varphi^2 \zeta + 2i\xi^4 \zeta - 2i\xi^2 \zeta}. \tag{8}
$$

The frequency response of Eq. (8) is depicted in Fig. (3a) for three different values ζ, which constitutes the damping according to the absorber resistance R_A. At low damping values of R_A, which is indicated by the blue line, only one resonance peak is present. This means, with regard to Fig. 1b, that the channel between both pressure chambers represents a short-circuit and, thus, the absorber is dynamically in an idle state and, furthermore, is not interacting with the primary system. Consequently, the degree of freedom of the absorber is lost and, thus, the transfer function has only one resonance frequency according to the original, undamped primary system without the HMA at the dimensionless frequency $\xi = \dfrac{\omega}{\omega_P} = 1$. On the other hand, the green line shows the frequency response with a very high resistance R_A, which has now two resonance peaks. The fact that both subsystems, the primary system and the absorber system, have nearly the same natural frequency results in a split-up
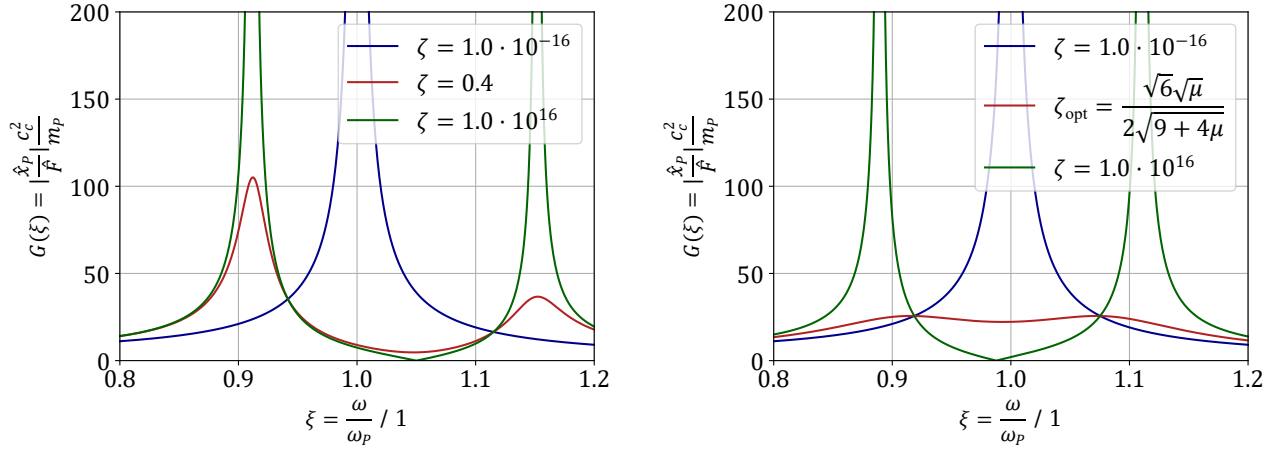
(a) Eq. (8) for 3 different damping values ζ at $\varphi = 1.05$ **(b)** red: optimized tuning φ_{opt} and damping ζ_{opt}

Figure 3: Transfer functions $G(s)$ of an HMA with $\mu = 0.05$ for different damping values ζ

of the single resonance peak into two eigenfrequencies, which are approximately mirrored around the dimensionless frequency $\xi = 1$. The third (red) curve in Fig. 3a shows a frequency response with a resistance value between both mentioned extremal values. It is remarkable that all three lines are passing through two distinct points, which are completely independent of the damping value ζ. They are called fixed points, which are located at the frequencies

$$\frac{\omega_I}{\omega_P} = \sqrt{\frac{\mu\varphi^2}{4} + \frac{\varphi^2}{2} - \frac{\sqrt{\mu^2\varphi^4 + 4\mu\varphi^4 + 4\mu\varphi^2 + 4\varphi^4 - 8\varphi^2 + 4}}{4} + \frac{1}{2}} \tag{9}$$

$$\frac{\omega_{II}}{\omega_P} = \sqrt{\frac{\mu\varphi^2}{4} + \frac{\varphi^2}{2} + \frac{\sqrt{\mu^2\varphi^4 + 4\mu\varphi^4 + 4\mu\varphi^2 + 4\varphi^4 - 8\varphi^2 + 4}}{4} + \frac{1}{2}}. \tag{10}$$

According to the design process from [7] the main strategy of the presented design paradigm is to bring both fixed points to the lowest possible level by an optimal tuning $\varphi = \frac{\omega_A}{\omega_P}$ and, furthermore, to place the maxima of the transfer function into these fixed points by adjusting the damping value ζ. For the considered primary system with the HMA this method succeeds with the optimal tuning

$$\varphi_{\text{opt}} = \sqrt{\frac{2}{\mu + 2}} \tag{11}$$

and the optimal damping

$$\zeta_{\text{opt}} = \frac{1}{2}\sqrt{\frac{6\mu}{4\mu + 9}}, \tag{12}$$

which is illustrated by the red curve in Fig. 3b. The resulting maximum magnitude calculates to

$$|G_{\text{opt}}|_{\text{max}} = 4\sqrt{\frac{2 + \mu}{\mu}}. \tag{13}$$

Using Eq. (11), the optimal mean operating pressure in the HMA calculates to

$$\overline{p} = \left(\frac{V_A m_A \left(p_0^G\right)^{\frac{1}{n}}}{\left(\frac{m_A}{m_P} + 2\right) A_p^2 n} \omega_P^2 \right)^{\frac{n}{n+1}}, \tag{14}$$

which, in case of $\mu = \frac{m_A}{m_P} = 0$, tends to the result of Eq. (3). Since in most cases $\mu \ll 1$ is valid, it becomes obvious that the operating pressure $\overline{p}$ is robust with respect to the optimal tuning, which simplifies a proper design of the absorber significantly. With regard to Eq. (12) the relation for the resistance R_A reads

$$R_A = \frac{m_P}{A_p^2} \sqrt{\frac{6\mu}{4\mu + 9}} \omega_P. \tag{15}$$

In hydraulics a linear resistance is not easy to realize, rather the quadratic characteristics of an orifice. Since the orifice equation is nonlinear with respect to the pressure drop Δp, an operating point of the intended resistance must be considered, like

$$q = \frac{\Delta p}{R_A} = Q_N \sqrt{\frac{\Delta p}{p_N}}. \tag{16}$$

The pressure drop Δp in the operating point can be assessed by evaluating the transfer function for the chamber pressure due to the excitation force

$$G_p(\xi) = \frac{\hat{p}}{\hat{F}} A_p = \frac{i\mu\varphi^2\xi^2\zeta}{2i\mu\varphi^2\xi^2\zeta - \mu\varphi^2\xi^3 + \mu\varphi^2\xi + 2i\varphi^2\xi^2\zeta - 2i\varphi^2\zeta - 2i\xi^4\zeta + 2i\xi^2\zeta} \tag{17}$$

according to the system dynamics from Eq. (5). Using again the conditions for optimal tuning and optimal damping from Eqs. (11) and (12), then the maximum dynamic pressure magnitude in a pressure chamber calculates to

$$\tilde{p}_{\max} = \frac{1}{A_p} \sqrt{\frac{12\left(\mu + 2\right)\left(\mu + 3\right)}{56\mu^2 + 255\mu + 288}} F, \tag{18}$$

which can be used for solving Eq. (16) for the nominal valve size

$$Q_N = \frac{\sqrt{2\tilde{p}_{\max} p_N}}{R_A}, \tag{19}$$

which in turn can be realized by a type of proportional valve orifice. Finally, the order of magnitude of the power dissipation over the resistance R_A can be assessed by

$$\overline{P} = \frac{1}{T} \int_0^T q_{R_A}(t) \Delta p(t) dt \approx 4 \frac{\tilde{p}_{\max}^2}{R_A}, \tag{20}$$

which is converted into heat.

4. SIMULATIONS

The dynamic behaviour of the absorber design is investigated by simulations as presented in the following. On the one hand the response due to an external excitation is analyzed, which is the most likely case in industrial applications. On the other hand the response resulting from a moderate instability in form of a negative damping value c_P of the primary system is shown.
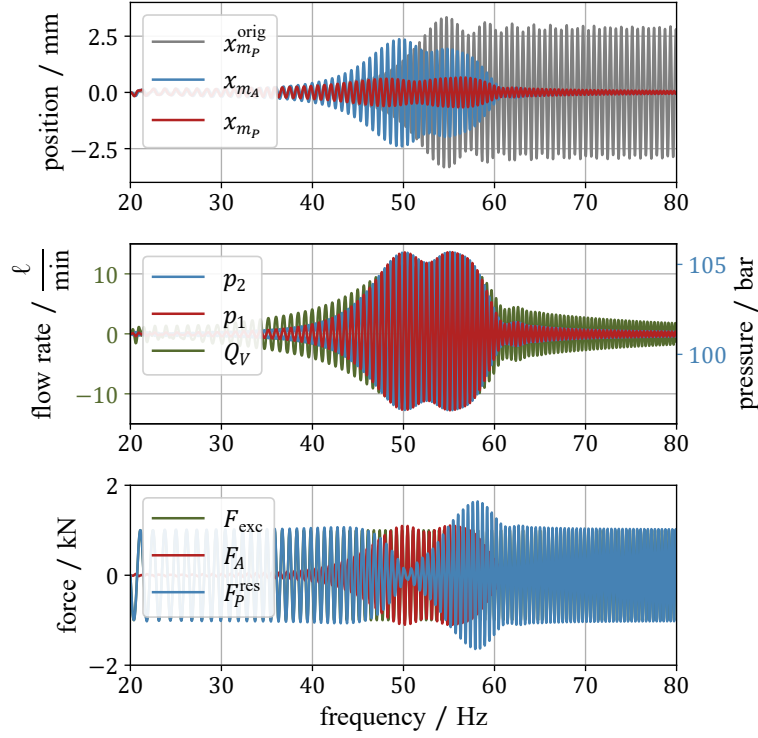
Figure 4: Response due to an external chirp excitation force F

4.1. External Excitation

In the simulation results presented in Fig. 4 the nonlinear system from Eq. (4) was excited by a chirp modulated force F_{exc} in order to investigate the system behaviour in a certain frequency range. In the upper diagram the grey signal $x_{m_P}^{orig}$ indicates the displacement of the primary mass without an absorber. The resonance frequency is designed to 50 Hz, thus, in this frequency range the magnitude is growing. In the simulations no viscous damping is considered for the primary system ($c_P = 0$). For this reason the magnitude remains constant at frequencies above the natural frequency of the primary system, since no power is dissipated. It must be remarked that in the simulations the chirp process was carried out within a simulation time of 2 seconds for illustration purposes. Thus, for a slower frequency rate a larger magnitude in the position $x_{m_P}^{orig}$ must be expected. The red line x_{m_P} in the upper diagram shows the displacement magnitude of the primary mass with the absorber and the blue signal x_{m_A} represents the magnitude of the absorber displacement. In the middle diagram the pressures in both absorber chambers as well as the flow rate through the damping resistance are illustrated. In the lower diagram the excitation force, the reaction force from the absorber and the resulting force on the primary mass as the sum from the excitation and the absorber are depicted.

The simulations taught that the system with the hydro-mechanical vibration absorber is well damped in the relevant frequency range. Furthermore, comparing the displacement of the damped primary mass in the upper diagram of Fig. 4 with the frequency responses in Fig. 3b, the maxima of the red optimized curve below and beyond the natural frequency of the primary system ($\xi = \dfrac{\omega}{\omega_P} = 1$) can be clearly identified. Thus, the nonlinear dynamics reflect the assumptions for the linear design process. However, this might not be the case anymore, if the excitation force exceeds a certain magnitude, which is not discussed in this contribution. According to Eq. (20) derived from the linear model the mean power dissipated over the resistance R_A is assessed to approximately 88 W and the measured dissipation power from the simulation with the nonlinear model results in approximately 95 W, which is in fact the same order of magnitude, but so far it cannot be assured that this holds for other dimensions.
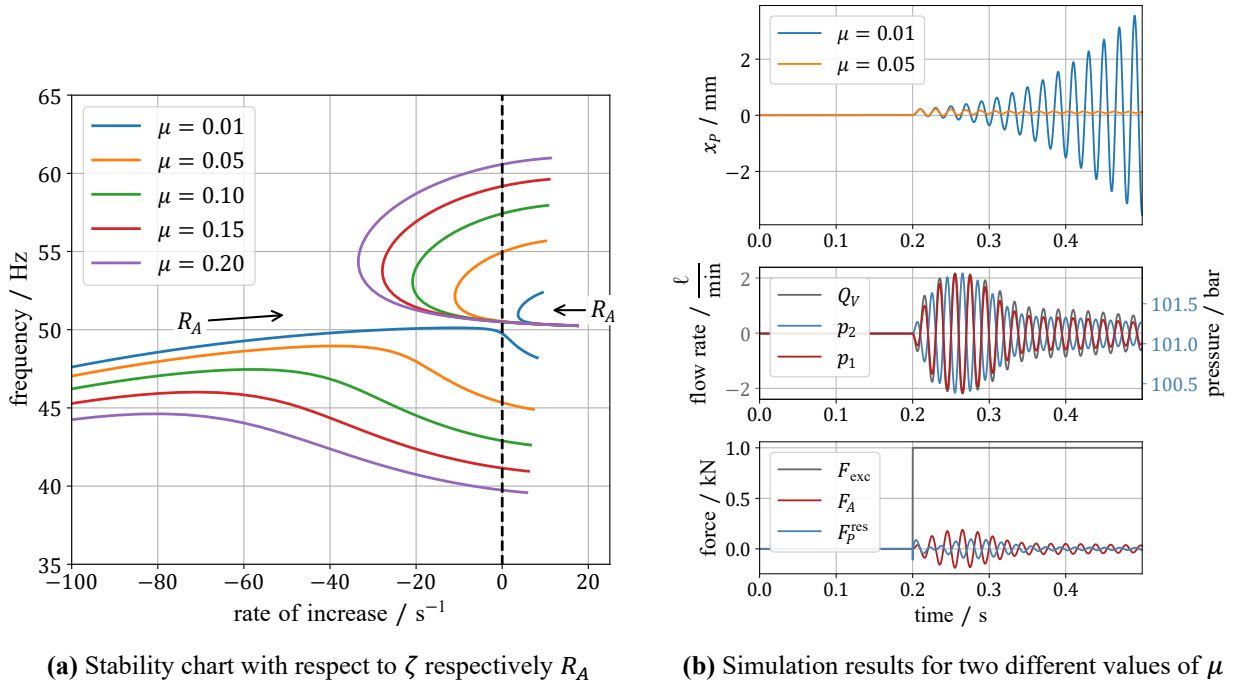
(a) Stability chart with respect to ζ respectively R_A

(b) Simulation results for two different values of μ

Figure 5: Unstable primary system with negative viscous damping c_P

4.2. Moderate Instability

In some applications a structural instability may lead to growing oscillations, like illustrated by the blue line in the upper diagram of Fig. 5b for the displacement of the primary mass x_P, which is caused by a negative damping of the primary system $c_P = -3500\,\frac{\text{Ns}}{\text{m}}$. In Fig. 5a the stability of the system at different mass ratios μ with regard to the damping resistance $R_A = 0, \dots, 10^{12}\,\frac{\text{Pa·s}}{\text{m}^3}$ is analyzed. Positive abscissa values denote the unstable region. At a resistance value $R_A = 0$ the system is unstable and oscillates at approximately $50\,\text{Hz}$ with a diverging magnitude. Increasing R_A results in a reduced rate of increase, however, when the absorber mass ratio is too low ($\mu = 0.01$) the system cannot be stabilized at all. With a larger absorber mass like, for instance, with $\mu = 0.05$ the instability due to the negative damping can be prevented with certain values of R_A. But, if the value of the resistance is increased further, then the system is becoming unstable again with different frequencies, which also occurs with larger absorber masses.

5. DISCUSSION

The basic structure of the HMA is a resonating mass between two pressure chambers and in case of need two mechanical springs. Basically, the resonance frequency is determined by the relation of mass and resulting stiffness of the different springs. Both pressure chambers are equipped with gas-loaded accumulators and their stiffness is adjusted by the mean operating pressure of the gas spring resulting in an adaptive natural frequency.

The absorber is encapsulated in a closed housing, which is mounted to the primary system to be dampened. The momentum of the absorber mass is converted to pressures in both chambers and the reactive force is transmitted by the housing, which must be designed significantly stiffer than the rigidity of the resulting parallel arrangement of the mechanical and gaseous springs.

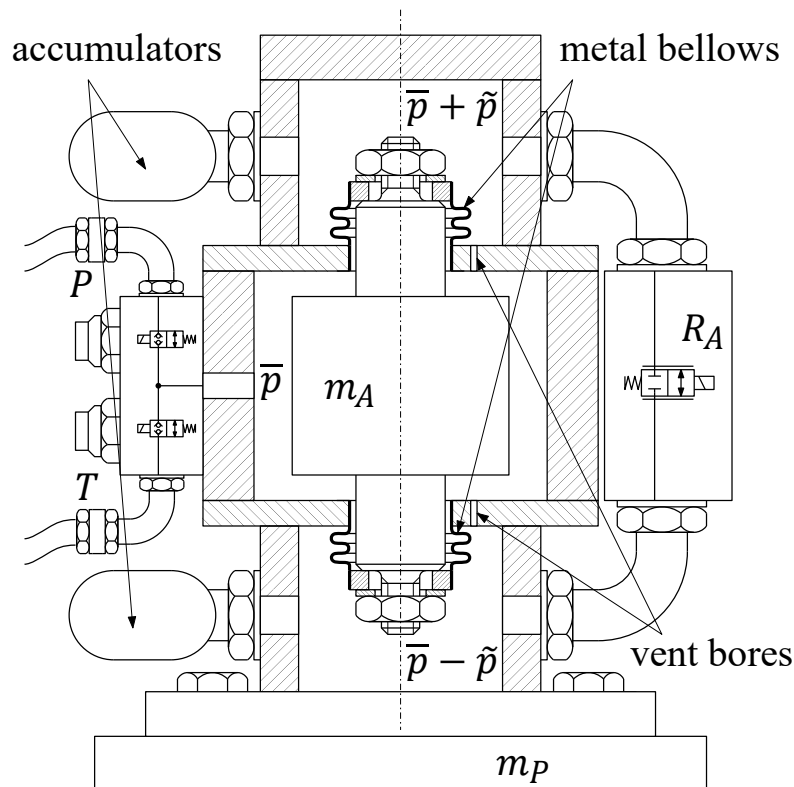In the absorber concept from Fig. 1b the piston is gliding in a sleeve, which is lubricated by the dy-

Figure 6: A realization study

namic leakage flow through the annulus gaps with the cross-sectional areas $A_\odot$. In the design procedure presented above, this leakage flow was completely neglected, however, the cross-sectional areas $A_\odot$ must be related to the nominal flow coefficient of the resistance R_A. Because, the clearance for lubrication and/or due to manufacturing tolerances between piston and sleeve may result in a considerable damping effect. Thus, the value of the resistance R_A must be obviously increased, which in turn can lead to very small and sensitive openings in the resistance valve. In order to avoid the problem of too high cross-sectional areas $A_\odot$ a different design for an exemplary realization of an HMA is depicted in Fig. 6, where the absorber mass is supported by two metal bellows for guiding the piston and sealing the chambers. The mean pressure in the absorber is adjusted by two seat-type valves for increasing or decreasing the operating pressure $\overline{p}$, which propagates now through vent bores from the centered mean pressure chamber to both dynamic pressure chambers. The dimension of the vent bores can be designed independently from the absorber design, since requirements for guiding and lubrication can be dropped. Furthermore, in many cases the dynamic displacement of the absorber mass is in the sub-millimeter range, thus, the major design restrictions for the metal bellows are the dynamic pressure $\tilde{p}$ and the gravity force of the absorber mass. In such a case, the metal bellows do not significantly contribute to the main stiffness of the absorber ($k_M \ll k_H$), which is determined mainly by the gas springs in the pressure chambers. However, the soft metal bellows are still able to maintain the mean center position of the absorber mass. For applications where the operating frequency varies a control of the mean operating pressure $\overline{p}$ is necessary. For applications with one constant operating frequency, a hydraulic supply is not even required, because the absorber is pressurized just once during the installation.

The higher the magnitude of the external excitation force, the higher the expected magnitudes of the dynamic states in the absorber, i.e., larger displacement of the absorber mass and larger dynamic pressure values $\tilde{p}$. The assessment of the dynamic states presented in the considerations above require the knowledge or at least the order of magnitude of the excitation force, which must be somehow identi-

fied by corresponding measurements. The assessment of the dissipated power according to Eq. (20) leads to lower values compared to the simulations with the nonlinear systems dynamics, but the order of magnitude is similar. If already the assessed power dissipation at the resistance R_A is considerably high, then a cooling strategy could be necessary.

In some applications the excitation frequency varies during operation. Basically, the optimal damping according to Eq. (12) leads to a robust system behaviour with regard to the excitation frequency like illustrated in Fig. 3b. But this is not true anymore, when the natural frequency of the primary system varies, which can occur in certain applications. In such a case the resonating frequency of the absorber and, thus, the mean operating pressure $\bar{p}$ must be adapted in order to maintain an optimized behaviour. There exist different strategies for adapting the operating point, which are out of scope of this contribution, however, in such a case a hydraulic supply and a signal processing unit are required. Then additional pressure transducers can be applied directly to the different pressure chambers in order to observe the effectiveness of the absorber.

The final paragraph is devoted to the potential applicability of the presented absorber. Since it is encapsulated in a closed housing, the absorber can be easily assembled to any vibrating spring mass system independent of the environmental conditions. Only the suitable oil temperature could be a limitation for certain applications, but also in such cases probably cooling or even heating could be an opportunity. If applied to a vibrating structure, then the absorber must be located in an antinode of resonance in order to achieve its best performance. Basically, the concept is not limited in size or frequency, however, the smaller the dimensions of the absorber the higher the influence of parasitic effects like, for instance, manufacturing tolerances or friction effects. Furthermore, if commercial components are used for the realization, then also the available dimensions may play certain role. But, compared to conventional absorbers the additional parameters of the variable hydraulic stiffness give much room and flexibility in the design process, which makes the concept interesting for a wide range of applications.

6. CONCLUSION AND OUTLOOK

In this paper the basic concept of a hydro-mechanic vibration absorber with adjustable operating frequency was presented. The absorber consists of a lumped mass resonating between two pressure chambers with an adjustable stiffness depending on the mean operating pressure. The nonlinear spring characteristics are realized by the gas springs of hydraulic accumulators, where the compressibility of the oil can be completely neglected. The main design aspects were derived mathematically and, furthermore, the considerations for optimal tuning and damping based on linear systems theory were carried out with regard to the established literature. Simulation experiments taught that the basic functionality of the absorber could be shown in the more realistic case of nonlinear system dynamics. Moreover, the stabilizing effect of the absorber for an unstable primary system could be demonstrated. The major design aspects for a realistic application as well as the assessment of dissipated power were discussed elaborately. A realization of a prototype and the verification of the concept by measurements constitute next steps in development. Furthermore, a strategy for an online adaption of the operating frequency is part of future work.

REFERENCES

[1] Ioi T, Ikeda K (1978) On the dynamic vibration damped absorber of the vibration system. Bulletin of JSME 21(151):64–71, DOI 10.1299/jsme1958.21.64

[2] Yuen T, Balan L, Mehrtash M (2019) Implementation of an Absorber Design for Vibration Control in Automation Systems. Procedia Manufacturing 32:578–584, DOI 10.1016/j.promfg.2019.02.255

[3] Bschorr O, Raida HJ (2022) One-Way Vibration Absorber. Acoustics 4(3):554–563, DOI 10.3390/acoustics4030034

[4] Wang M, Xu H, He D, Wang T, Zhang J (2022) Design of a damped vibration absorber to control the resonant vibration of roll. Mechanical Systems and Signal Processing 178:109,262, DOI 10.1016/j.ymssp.2022.109262

[5] Trujillo-Franco LG, Flores-Morita N, Abundis-Fong HF, Beltran-Carbajal F, Dzul-Lopez AE, Rivera-Arreola DE (2022) Oscillation Attenuation in a Building-like Structure by Using a Flexible Vibration Absorber. Mathematics 10(3):289, DOI 10.3390/math10030289

[6] Daman AAA, Guntur HL, Susastro (2016) The influence of dynamic vibration absorber to reduce the vibration of main system with 2-DoF. In: AIP Conference Proceedings, Author(s), DOI 10.1063/1.4965762

[7] Den Hartog JP (1947) Mechanical Vibrations. McGraw-Hill Boo Company, Inc.

[8] Esen I, Koc MA (2015) Optimization of a passive vibration absorber for a barrel using the genetic algorithm. Expert Systems with Applications 42(2):894–905, DOI 10.1016/j.eswa.2014.08.038

[9] Hao Y, Shen Y, Li X, Wang J, Yang S (2020) H_∞ optimization of Maxwell dynamic vibration absorber with multiple negative stiffness springs. Journal of Low Frequency Noise, Vibration and Active Control 40(3):1558–1570, DOI 10.1177/1461348420972818

[10] Yuan M, Jin Y, Liu K, Sadhu A (2022) Optimization of a Non-Traditional Vibration Absorber for Vibration Suppression and Energy Harvesting. Vibration 5(3):383–407, DOI 10.3390/vibration5030022

[11] Guo X, Zhu Y, Qu Y, Cao D (2022) Design and experiment of an adaptive dynamic vibration absorber with smart leaf springs. Applied Mathematics and Mechanics 43(10):1485–1502, DOI 10.1007/s10483-022-2905-6

[12] Punyakaew S (2022) Adaptively tuned vibration absorber using cone based continuously variable transmission. Cogent Engineering 9(1), DOI 10.1080/23311916.2022.2102044

[13] Rincon CG, Alencastre J, Rivera R (2021) Active Vibration Absorber for a Continuous Structure Model. engrXiv (Engineering Archive) DOI 10.31224/osf.io/r3ujn

[14] Timorian S, Valasek M (2022) Dual Frequency Vibration Absorber. In: Computational Mechanics 2022, University of West Bohemia

[15] Zhang J, Xie F, Ma Z, Liu XJ, Zhao H (2023) Design of parallel multiple tuned mass dampers for the vibration suppression of a parallel machining robot. Mechanical Systems and Signal Processing 200:110,506, DOI 10.1016/j.ymssp.2023.110506